# Is a blunt sword pointless? Tooth wear impacts puncture performance in Tasmanian devil canines

Tahlia I. Pollock[1,2,*], David P. Hocking[2,3], and Alistair R. Evans[2,4]

[1]The Palaeobiology Research Group, School of Earth Sciences, University of Bristol, Bristol, UK
[2]School of Biological Sciences, Monash University, Melbourne, Australia
[3]Department of Zoology, Tasmanian Museum and Art Gallery, Hobart, Australia
[4]Museums Victoria Research Institute, Museums Victoria, Melbourne, Australia

[*]Author for correspondence: tahliaipollock@gmail.com

TIP: orchid – https://orcid.org/0000-0001-5605-9069 e – tahliaipollock@gmail.com
DPH: orchid – https://orcid.org/0000-0001-6848-1208 e – david.hocking@tmag.tas.gov.au
ARE: orchid – https://orcid.org/0000-0002-4078-4693 e – alistair.evans@monash.edu

As teeth wear, their shapes change and functional features can be dulled or lost, presumably making them less effective for feeding. However, we do not know the magnitude and effect of this wear. Using Tasmanian devil canines as a case study, we investigate the impact of wear on puncture in pointed teeth. We measured aspects of shape impacted by wear (tip sharpness, height, and volume) in teeth of varying wear followed by 3D printing real and theoretical forms to carry out physical puncture tests. Tooth wear acts in two ways: by blunting tooth tips, and decreasing height and volume, both of which impact performance. Sharper tips in unworn teeth decrease the force and energy required to puncture compared to blunter worn teeth, while taller unworn teeth provide the continuous energy necessary to propagate fracture relative to shorter worn teeth. These wear-modulated changes in shape necessitate more than twice the force to drive worn teeth into ductile food and decrease likelihood of puncture success.

**Keywords:** tooth wear, tooth morphology, puncture performance, mammal, canine

## Introduction

Throughout an animal's lifetime, their teeth will experience countless interactions with food items and opposing teeth causing them to wear. As teeth wear, their shape changes and

functional features can be dulled or lost altogether [1-3]. Once sharp blades may become ineffective at cutting through plant material or previously elongate pointed teeth may struggle to puncture prey. However, this has not been quantified experimentally and the magnitude and effect of this wear on tooth performance is not known.

Often the first point of contact between predator and prey, canine teeth are used to bite into a range of tissues. During feeding, canines may encounter one or a combination of grit-covered hides, flesh and bone, exoskeleton, hard-shelled prey, and even fibrous plant materials, each causing wear [1, 4-8]. As a canine tooth wears, the sharp tip (and sometimes edges) will blunt, tooth height and volume decrease, and robustness increases [1, 9]. Previous research shows that tooth tip sharpness, volume, and robustness impact puncture performance [3, 10-13]. As tools primarily used for puncture, canine teeth represent an excellent study system to investigate the relationship between tooth wear and performance. While the impact of tooth wear is expected to be especially important for older individuals, breakage and subsequent wear can happen to carnivores at all stages of life and in effect speed-up tooth wear [14]. Due to their elongate form, canine teeth are the most frequently broken tooth in a carnivore's tooth row [1]. Hence, understanding the 'cost' of a worn or broken canine is of particular importance.

Here, we quantify aspects of tooth shape impacted by wear in Tasmanian devil (*Sarcophilus harrisii*) canines. Devils are an ideal candidate, as their diet and feeding behaviours expose their teeth to high wear, the degree and range of which is well documented [15-21]. To experimentally quantify the relationship between tooth wear and performance we 3D printed a series of real and theoretical canine forms of varying wear states and subjected them to physical puncture tests.

## Materials and methods

### *Quantifying tooth wear*

We selected 38 Tasmanian devil canine teeth that spanned the range of tooth wear variation documented in the literature [19, 21-23]. Teeth were sourced from multiple museum collections (Museums Victoria NMV, the Tasmanian Museum and Art Gallery TMAG, and the Australian Museum AMS). Each tooth was coded according to a pre-existing tooth wear index and assigned to one of the five wear categories [21] (Supplementary Materials Table S1).

For digitisation, specimens were moulded and cast with silicone rubber impression material (Flexitime Correct Flow A-silicone; Heraeus, Germany) and gypsum dental stone

(Alpha-rock golden brown premium quality gypsum; AlphaBond Dental, Australia). Casts were scanned on a Laser Design DS-Series 2025 3D scanner with an RPS-120 laser probe (620 nm) at a point spacing of 10 um. Point clouds generated were merged into a single mesh in Geomagic Wrap 2015 (Geomagic, Santa Clara, USA).

Tooth shape measurements were taken in Rhinoceros 5 (McNeel North America, USA). We measured tooth height from the tip of the tooth to the highest point of the boundary of the enamel, tooth width at the base of the tooth, and calculated tooth volume. We also quantified the surface area of the tip of the tooth at a distance of 2 mm from the tip (*SA*2mm) and the volume of the tip of the tooth at a distance of 5 mm from the tip (*V*5mm). By measuring tip surface area, we are quantifying the amount of a tooth's surface in contact with the substrate, which previous research on puncture mechanics has identified as important for force transmission and stress, which impact crack initiation [3, 11, 24, 25]. The smaller the surface area of tooth in contact with the substrate, the higher the stress for a given force and more likely fracture. Additionally, measuring tip volume (*V*5mm) and tooth volume enables us to quantify the amount of tooth being driven into the substrate and so the amount of substrate that needs to deform or be displaced, which has been highlighted as important for continued penetration [3, 11]. The less substrate that needs to be deformed or displaced the fewer atomic bonds in the material need to break to continue penetration. We expect that our measures of tip sharpness (*SA2*mm and *V*5mm) will be highly correlated; however, the inclusion of tip volume allows us to examine the relationship between volume and puncture independent of tooth height in our controlled initial puncture experiments (described below), which is not the case for total tooth volume. Together these metrics capture the aspects of tooth shape impacted by wear: tip sharpness (*SA*2mm and *V*5mm), tooth height, volume, and robustness (tooth height/tooth width) (Figure. 1). Focusing on a single tooth within a model species allows us to experimentally control for size related differences in our measures of tooth shape, and so we use absolute values. However, when comparing measures of tooth shape across taxonomically broad datasets with disparate body sizes applying a scaling factor or using scale independent measures of shape would be more appropriate, especially for sharpness [8, 10, 26, 27].

*Model creation and 3D printing*

Theoretical tooth models were created that span the variation in wear observed (Fig. 1; Supplementary Materials Fig. S1). Models were generated in Rhinoceros 5 by selecting a single unworn tooth (museum specimen NMV C3242) and artificially wearing it by removing

tooth height at specific intervals (5% of the tooth height, 10%, 15%, 20%, 30%, 40%, and 50%). To simulate the worn tip, we generated a surface from the equation $y = 0.5\ x^{0.2}$, taken from [28] which describes a blunt tipped pointed tooth. This was scaled and trimmed to fit the cut tooth and then merged in Geomagic to create the final theoretical model. Tooth shape metrics were measured for all theoretical models.

All theoretical models (8 total), and 8 real models (generated from the casts of museum specimens) were chosen for 3D printing and puncture testing. For each theoretical tooth model, we selected one real tooth model which has the most similar tip sharpness value (*SA*2mm) resulting in tooth models representing wear states: W0, W5, W10, W15, W20, W30, W40, and W50. To enable secure mounting and a consistent run length (total displacement) for puncture tests, tooth models were designed to have a 18 x 30 x 12 mm base block and a total height of 30 mm. Tooth models were trimmed at their base so that the resulting edge was flat and perpendicular to the central axis of the tooth. However, as the heights of each tooth varied, to achieve the desired total model height (30 mm), the base edge of each model was extended via the 'extrude' function in Geomagic. The amount extruded differed for each tooth and was calculated by adding the block height (12 mm) and tooth height (e.g., 12.35 mm for museum specimen NMV C2652) and subtracting it from the desired model height (30 mm). Once each tooth edge was extruded the block was attached. One copy of each model was printed using a stereolithography (SLA) 3D printer, the Form 3 by Formlabs (USA) in Formlabs Standard Grey resin with a layer thickness of 0.050 mm. See Supplementary Materials Fig. S1 for model creation workflow.

*Puncture tests*

To remove the inherent variability of using a biological substrate like animal tissue, we used a gelatine analogue designed to mimic human skin and muscle tissue: Medical Gelatine #2 (Humimic Medical, USA). Material properties: Density 923.468ρ Kg/m³, Speed of Sound: 1457.42 m/s, Young's Modulus: 0.26 MPa, Firmness: 308 g, and Needle resistance: 0.38 N (Humimic website). Gelatine was moulded and cast into 50 x 50 x 50 mm blocks for puncture tests.

A Force Tester (Instron 5982 Universal Testing Machine, Instron, USA) with a S40A 50 kg load cell (HBM, Darmstadt, Germany) was used to measure the force (N) and displacement (mm) required by each tooth model to puncture the gelatine substrate. For each test, the tooth model was secured with a clamp attached to the load cell and the substrate placed on a platform below so that there was ~1 mm between substrate and tooth tip. The set-

up was designed so that the tooth moved downwards into the substrate at a constant speed of 2 mm/s for a distance of 18 mm, referred to as a 'run'. Between each run, tooth models were cleaned, and the substrate replaced. For all tooth models, we performed six replicates of each run. The force and displacement output were recorded at 10 measurements per second by the data logger program EVIDAS Essential (v. 1.3.0, HBM, Darmstadt, Germany).

To assess puncture success, for each replicate we photographed and visually inspected the gelatine block immediately after the run as well as 20 mins after the run.

*Analysis*

Force and displacement data for each replicate was processed and analysed in Excel (v. 16.74, Microsoft, USA) and using RStudio statistical and graphical environment (R v. 4.0.3, RStudio v. 1.3.1093,[29]). As previous research linked tip sharpness to the crack-initiation phase of puncture, and tool height and volume to the continued penetration phase, we separated our analyses into two parts [3, 11, 30]. First, to assess how tooth wear impacts initial contact/fracture between tooth and substrate, we calculated the maximum force (N) and energy (Nmm; calculated as the area under the force displacement curve) for each tooth model for the first 5 mm of the run (displacement 5 mm) and plotted these against measures of sharpness (*SA*2mm and *V*5mm). Then, to assess how tooth wear impacts the complete bite/continued penetration, we calculated the maximum force and energy to a displacement equivalent to the tooth height of each model and plotted against tooth height, tooth volume, and tooth robustness (tooth height/ tooth width), respectively. For each tooth model, maximum force and energy values for each replicate were averaged. Puncture was recorded as successful if there was visible damage to the cube, and unsuccessful if there was no visible damage (when substrate deformed around the tooth but did not break).

**Results and discussion**

We observed two patterns between tooth wear and puncture performance. For initial contact/fracture (displacement of 5 mm), as tooth wear increases (tips becoming blunter) so does the maximum force and energy (Fig. 2a-f), with significant positive correlations observed in real and theoretical tooth models for all sharpness metrics ($R^2 > 0.82$, $p < 0.01$; see Supplementary Materials Table S3 for full output of all statistical tests). For the *SA*2mm sharpness metric, having a very worn tip compared to an unworn tip increased maximum puncture force by approximately 240%, where our highest wear theoretical (THEO_50) and real (REAL_50) tooth models required 1.11 N and 1.09 N, respectively and our unworn

theoretical (THEO_0) and real (REAL_0) tooth models required 0.40 N and 0.45 N, respectively. In theoretical models, for a 30.11 $mm^2$ increase in bluntness (*SA2*mm) we find a 0.71 N increase in puncture force (THEO_0 = 13.10 $mm^2$ and THEO_50 = 43.21 $mm^2$) and for real models a 34.88 $mm^2$ increase in bluntness increases force by 0.64 N (REAL_0 = 13.34 $mm^2$ and REAL_50 = 48.22 $mm^2$). A similar pattern was observed for sharpness metric *V*5mm (see Supplementary Materials Table S2).

In contrast, for the complete bite/continued penetration (displacement equivalent to tooth height), as tooth wear increases (heights and volumes decreasing and robustness increasing) maximum force and energy decreases (Fig. 2g-l), with significant negative correlations observed for tooth height in real and theoretical tooth models ($R^2 > 0.70$, $p < 0.01$; see Supplementary Materials Table S3 for full output of all statistical tests) and also for tooth volume in theoretical ($R^2 > 0.95$, $p < 0.01$) but not real tooth models ($p > 0.05$). Having a very worn tooth compared to an unworn tooth decreased the maximum puncture force by approximately 130%, where our highest wear theoretical (THEO_50) and real (REAL_50) tooth models required 1.72 N and 1.54 N, respectively, and our unworn theoretical (THEO_0) and real (REAL_0) tooth models required 2.37 N and 2.03 N, respectively. In theoretical models, for a 6.61 mm decrease in tooth height we find a 0.65 N decrease in puncture force (THEO_0 = 13.10 mm and THEO_50 = 43.21 mm) and in real models a 6.52 mm decrease in tooth height decreases puncture force by 0.83 N (REAL_5 = 12.74 mm and REAL_50 = 6.22 mm; using REAL_5 in this instance as it has the highest height value). See Supplementary Materials Table S2 and Fig. S2 for tooth volume and tooth robustness.

For both real and theoretical tooth models, as wear increases, the likelihood of puncture decreased (Fig. 2). Unworn and lightly worn tooth models (W0 and W5) were observed to successfully puncture the substrate in all replicates, while heavy wear models (W40 and W50) did not puncture in any replicates. Models with intermediate wear (W10 – W30) displayed varying puncture success (Supplementary Materials Table S2).

Our results demonstrate experimentally the impact of tooth wear on puncture performance in pointed teeth. We show that wear acts two ways, by blunting tooth tips and decreasing the total tooth height and volume, all of which influence puncture performance.

During initial contact/fracture, increased wear and tip bluntness results in increased force and energy. For a given displacement (5 mm), the sharp tips of the less worn tooth models have a smaller surface area of contact with the substrate than the blunt tips of more worn teeth. This concentrates the force on a smaller surface area, resulting in increased stress in the substrate and likelihood of breaking the atomic bonds in the material [11, 24, 25, 31].

Previous work investigating relationships between shape and performance in pointed tooth forms have found the same general pattern between tip sharpness and puncture performance [3, 10, 12, 13, 32, 33]. However, we demonstrate it relative to tooth wear for the first time and are also able to show that, in Tasmania devil canine teeth, the approximately x3 increase in tip surface area (*SA2*mm) between an unworn tooth (W0) and a very worn tooth (W50) increases force by approximately x2.5.

We observed an inverse relationship between wear and puncture performance for the complete bite, where increased tooth wear (loss of tooth height and volume and increased robustness) decreased the force and energy needed. In ductile and tough materials like the medical gelatine used in this study and vertebrate skin and muscle, the applied force initially results in food deformation. Once initiated, a crack requires a significant amount of energy to propagate through the tough material [11, 25, 30, 34, 35]. As a tooth is pushed in, the material will continue to deform until the stress is sufficient to initiate a crack (initial fracture), and continued contact is necessary to propagate the crack (continued penetration) [11, 31]. In both these scenarios, if the tooth is not tall enough (or sharp enough), neither crack formation nor propagation will occur. Hence, we demonstrate that height is an important aspect of tooth shape related to puncture performance in animals that bite into ductile materials. Changes to canine tooth height, either from wear within a species or morphological differences between species (e.g., giant panda vs. a sabre-tooth like *Smilodon*), will likely impact puncture performance.

These wear-modulated changes in tooth features (sharpness, height, volume, and robustness) occur concurrently as a tooth wears throughout an animal's life; in combination, they make worn teeth less likely to successfully puncture prey. Put simply, there appears to be a minimum sharpness and tooth height required to initiate and propagate cracks in ductile and tough materials; worn teeth have neither, making them less effective. We see this borne out in the puncture success of our tooth models, where unworn and light wear models (W0 and W5) punctured in all replicates and very worn models (W40 and W50) did not puncture in any.

Tasmanian devils present a particularly interesting case study as, unusually for mammals, their canine teeth continue to erupt throughout their lives, and this over-eruption has been documented as a proxy for age [21, 22, 36-38]. Canine over-eruption in devils has been shown to maintain tooth height and may help compensate for their high wear diets (Jones *et al.* (in review)) and is an interesting avenue for future research to explore.

This study has quantified the magnitude of the effect of tooth wear, showing that worn teeth require more than twice the force to drive into ductile food, and in fact may not puncture the food. Therefore, there may be strong limits on feeding performance of individuals with worn teeth, reducing efficiency or requiring dietary change. Our findings have wide reaching implications for tooth performance in carnivores, for example, in older individuals, which are likely to have a higher degree of tooth wear, but also for carnivores at all stages of life which through tooth breakage and subsequent wear will be impacted [1, 14].

**Acknowledgements**

The authors wish to thank to Kathryn Medlock and Belinda Bauer (Tasmanian Museum and Art Gallery, Hobart Australia), Karen Roberts and Rickey-Lee Erickson (Museums Victoria, Melbourne Australia), and Sandy Ingleby and Harry Parnaby (Australian Museum, Sydney, Australia) for allowing access to specimens. Our additional thanks to Michelle Quayle and Lucy Costello (Monash 3D Printing, Melbourne Australia) for their help in 3D printing tooth models. We would also like to thank John Beadle (Department of Civil Engineering at Monash University, Melbourne Australia) for their expertise in facilitating the physical puncture tests. Our additional sincere thanks to Blaire Van Valkenburgh and one anonymous reviewer for their valuable feedback and comments on the manuscript.

**Funding**

This project was supported by the by The Holsworth Wildlife Research Endowment and The Ecological Society of Australia, the Australian Government Research Training Program Stipend, the Monash University Graduate Excellence Scholarship, the Monash University Graduate Research Completion Award, the Monash University Post Publication Award, the Monash University PhD Travel Grant, and the Monash University School of Biological Sciences PhD Travel Grant (TIP) in addition to an Australian Research Council Discovery Project Grant (grant no. DP180101797) (ARE).

**Data accessibility**

The datasets supporting this article have been uploaded as part of the Supplementary Materials. 3D printed model files are accessible via Monash Bridges on FigShare: https://figshare.com/s/7c3ff4cb9a182e1449ea

## References


1. Van Valkenburgh, B., *Incidence of tooth breakage among large, predatory mammals.* The American Naturalist, 1988. **131**(2): p. 291-302.
2. Evans, A.R., *Connecting morphology, function and tooth wear in microchiropterans.* Biological Journal of the Linnean Society, 2005. **85**(1): p. 81-96.
3. Evans, A. and G. Sanson, *The effect of tooth shape on the breakdown of insects.* Journal of Zoology, 1998. **246**(4): p. 391-400.
4. Ewer, R., *The Carnivores*. 1973, Ithaca, New York: Cornell University Press.
5. Van Valkenburgh, B., *Feeding behavior in free-ranging, large African carnivores.* Journal of Mammalogy, 1996. **77**(1): p. 240-254.
6. Van Valkenburgh, B. and C. Ruff, *Canine tooth strength and killing behaviour in large carnivores.* Journal of Zoology, 1987. **212**(3): p. 379-397.
7. Christiansen, P. and S. Wroe, *Bite forces and evolutionary adaptations to feeding ecology in carnivores.* Ecology, 2007. **88**(2): p. 347-358.
8. Pollock, T.I., D.P. Hocking, and A.R. Evans, *The killer's toolkit: remarkable adaptations in the canine teeth of mammalian carnivores.* Zoological Journal of the Linnean Society, 2021.
9. Van Valkenburgh, B. and F. Hertel, *Tough times at La Brea: tooth breakage in large carnivores of the late Pleistocene.* Science, 1993. **261**(5120): p. 456-459.
10. Crofts, S., et al., *How do morphological sharpness measures relate to puncture performance in viperid snake fangs?* Biology letters, 2019. **15**(4): p. 20180905.
11. Anderson, P.S., *Making a point: shared mechanics underlying the diversity of biological puncture.* Journal of Experimental Biology, 2018. **221**(22): p. jeb187294.
12. Freeman, P.W. and C.A. Lemen, *The trade-off between tooth strength and tooth penetration: predicting optimal shape of canine teeth.* Journal of Zoology, 2007. **273**(3): p. 273-280.
13. Freeman, P.W. and W.N. Weins, *Puncturing ability of bat canine teeth: the tip.* Mammalogy Papers: University of Nebraska State Museum, 1997: p. 9.
14. Van Valkenburgh, B., et al., *Tooth fracture frequency in gray wolves reflects prey availability.* Elife, 2019. **8**: p. 658468.
15. Andersen, G.E., et al., *Dietary partitioning of Australia's two marsupial hypercarnivores, the Tasmanian devil and the spotted-tailed quoll, across their shared distributional range.* PLoS One, 2017. **12**(11): p. e0188529.
16. Jones, M.E. and L.A. Barmuta, *Diet overlap and relative abundance of sympatric dasyurid carnivores: a hypothesis of competition.* Journal of Animal Ecology, 1998. **67**(3): p. 410-421.
17. Pemberton, D., et al., *The diet of the Tasmanian devil, Sarcophilus harrisii, as determined from analysis of scat and stomach contents.* Papers and Proceedings of the Royal Society of Tasmania, 2008. **142**(2): p. 13-22.
18. Pollock, T.I., et al., *Torn limb from limb: the ethology of prey-processing in Tasmanian devils (Sarcophilus harrisii).* Australian Mammalogy, 2021.
19. Pemberton, D., *Social organisation and behaviour of the Tasmanian devil, Sarcophilus harrisii [PhD thesis]*. 1990, University of Tasmania: Hobart.
20. Jones, M., *Guild structure of the large marsupial carnivores in Tasmania [PhD thesis]*. 1995, University of Tasmania: Hobart.
21. Pollock, T.I., et al., *Wearing the devil down: Rate of tooth wear varies between wild and captive Tasmanian devils.* Zoo Biology, 2021.

22. Jones, M.E., et al., *Life-history change in disease-ravaged Tasmanian devil populations.* Proceedings of the National Academy of Sciences, 2008. **105**(29): p. 10023-10027.
23. Lachish, S., H. McCallum, and M. Jones, *Demography, disease and the devil: life-history changes in a disease-affected population of Tasmanian devils (Sarcophilus harrisii).* Journal of Animal Ecology, 2009. **78**(2): p. 427-436.
24. Lucas, P., *Basic principles of tooth design.* Teeth: form, function and evolution. New York: Columbia University Press. p, 1982: p. 154-162.
25. Crofts, S., S. Smith, and P. Anderson, *Beyond description: the many facets of dental biomechanics.* Integrative and Comparative Biology, 2020. **60**(3): p. 594-607.
26. Evans, A.R., et al., *The scaling of tooth sharpness in mammals.* Annales Zoologici Fennici, 2005. **42**(6): p. 603-613.
27. Hocking, D.P., et al., *Ancient whales did not filter feed with their teeth.* Biology letters, 2017. **13**(8): p. 20170348.
28. Evans, A.R., et al., *A universal power law for modelling the growth and form of teeth, claws, horns, thorns, beaks, and shells.* BMC biology, 2021. **19**(1): p. 1-14.
29. R Development Core Team, *R: A language and environment for statistical computing*. 2018, R Foundation for Statistical Computing. Retrieved from http://www.R-project.org: Vienna, Austria.
30. Lucas, P.W., *Dental functional morphology: how teeth work*. 2004, Cambridge: Cambridge University Press.
31. Lucas, P. and D. Luke, *Chewing it over: basic principles of food breakdown*, in *Food acquisition and processing in primates*. 1984, Springer Sciences: New York. p. 283-301.
32. Freeman, P.W., *Canine teeth of bats (Microchiroptera): size, shape and role in crack propagation.* Biological Journal of the Linnean Society, 1992. **45**(2): p. 97-115.
33. Whitenack, L.B. and P.J. Motta, *Performance of shark teeth during puncture and draw: implications for the mechanics of cutting.* Biological Journal of the Linnean Society, 2010. **100**(2): p. 271-286.
34. Freeman, P.W. and C. Lemen, *Puncturing ability of idealized canine teeth: edged and non-edged shanks.* Journal of Zoology, 2006. **269**(1): p. 51-56.
35. Evans, A.R. and S. Pineda-Munoz, *Inferring Mammal Dietary Ecology from Dental Morphology*, in *Methods in Paleoecology: Reconstructing Cenozoic Terrestrial Environments and Ecological Communities*, D.A. Croft, D.F. Su, and S.W. Simpson, Editors. 2018, Springer International Publishing: Cham. p. 37-51.
36. Lachish, S., M. Jones, and H. McCallum, *The impact of disease on the survival and population growth rate of the Tasmanian devil.* Journal of Animal Ecology, 2007. **76**: p. 926-936.
37. Lazenby, B.T., et al., *Density trends and demographic signals uncover the long-term impact of transmissible cancer in Tasmanian devils.* Journal of Applied Ecology, 2018. **55**(3): p. 1368-1379.
38. Bell, O., et al., *Age-related variation in the trophic characteristics of a marsupial carnivore, the Tasmanian devil Sarcophilus harrisii.* Ecology and Evolution, 2020. **10**(14): p. 7861-7871.

# Figures

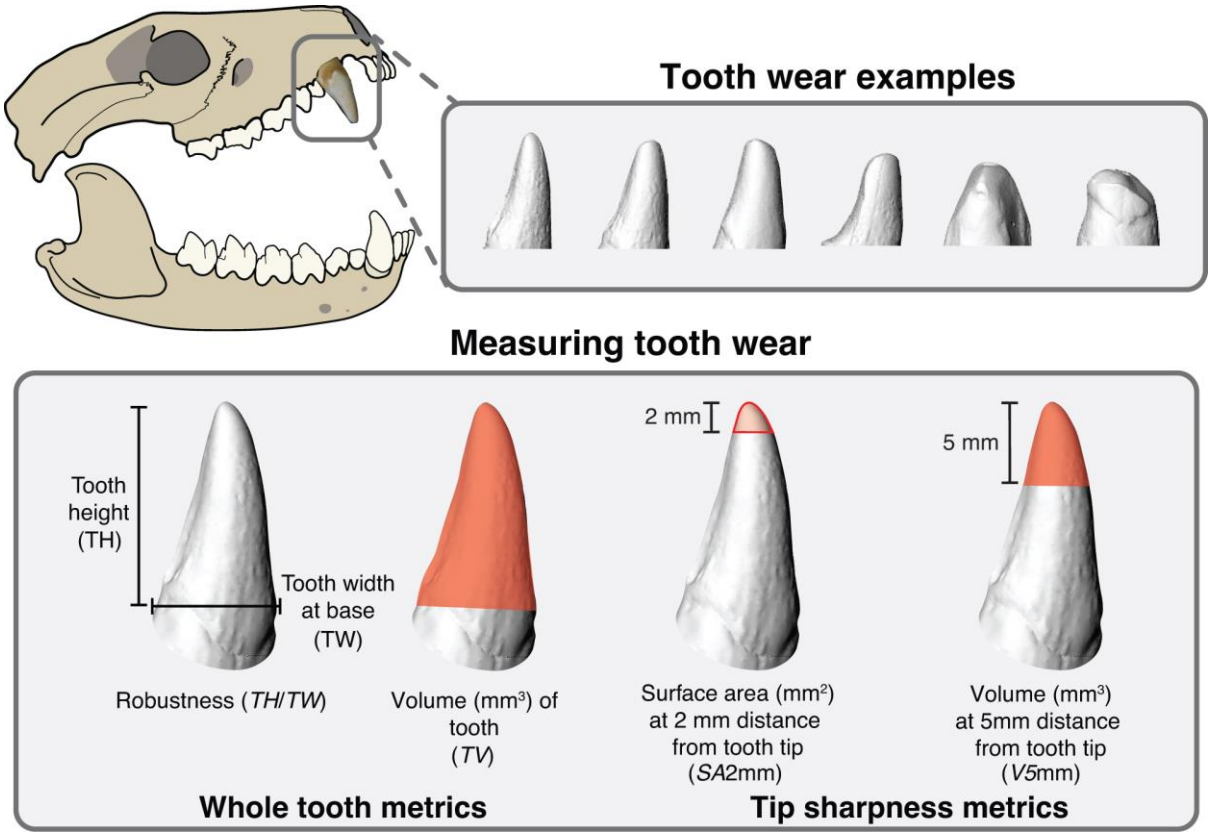


**Fig. 1.** Tooth wear examples in Tasmanian devil *Sarcophilus harrisii* and tooth shape metrics used to capture aspects of wear in this study. Tooth height (*TH*), robustness (*TH*/*TW*), volume (*TV*), and tip sharpness (*SA*2mm and *V*5mm).

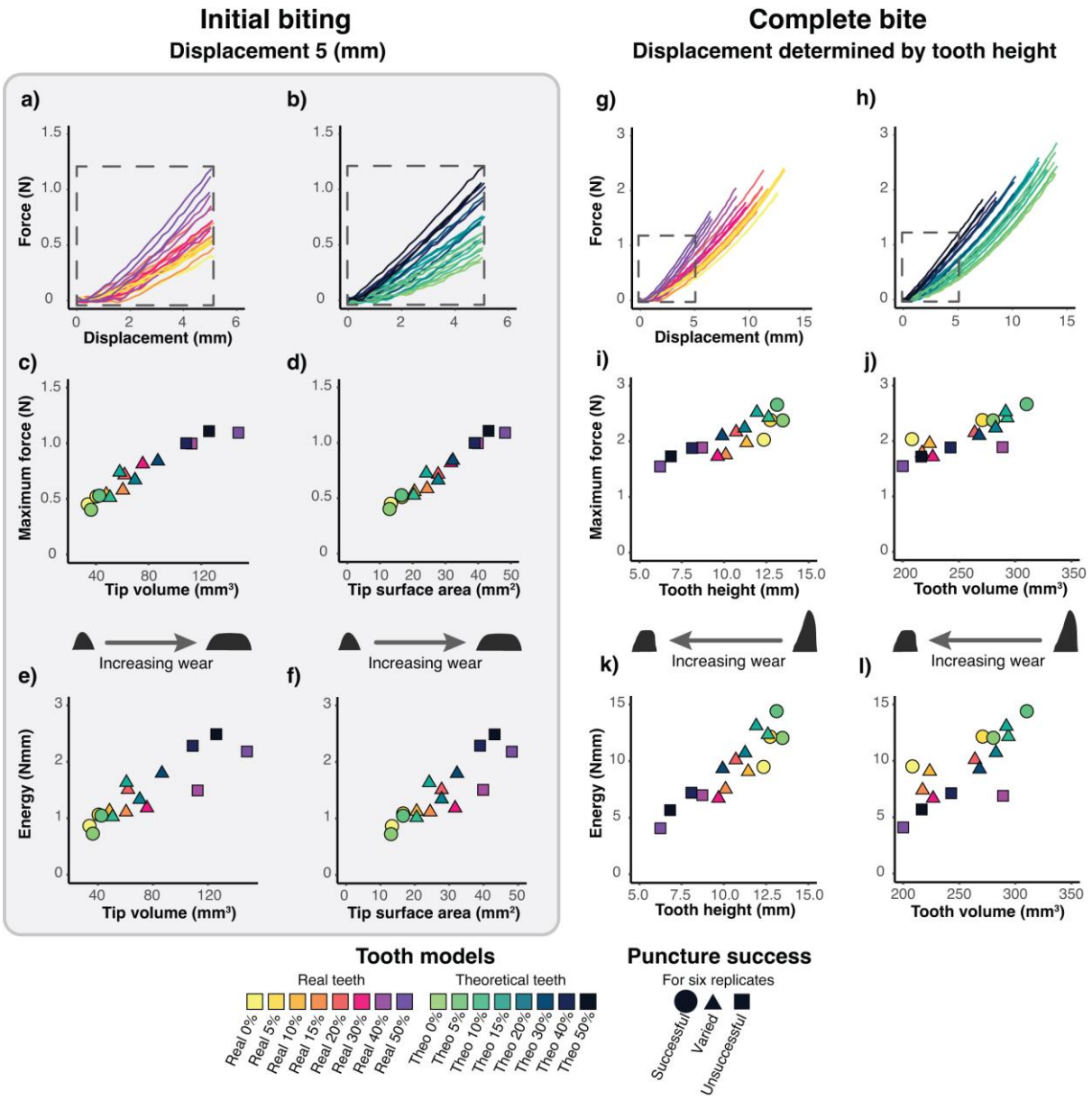


**Fig. 2.** Puncture performance results for initial biting (a-f) and complete bite analyses (g-l), showing the force (N) vs. displacement (mm) traces for all replicates trimmed to the first 5 mm of the run (a and b) and for the full height of each tooth model (g and h). For penetration of the first 5 mm, maximum force (N) (c and d) and energy (Nmm) (e and f) increase with wear metrics (tip volume, $mm^3$ and tip surface area, $mm^2$). For complete tooth penetration, both maximum force (i and j) and energy (k and l) decreased with wear (tooth height, mm and tooth volume, $mm^3$). Real tooth models (Real) and theoretical tooth models (Theo) at eight wear states (0% to 50%). Shapes denote combined puncture success for all replicates.

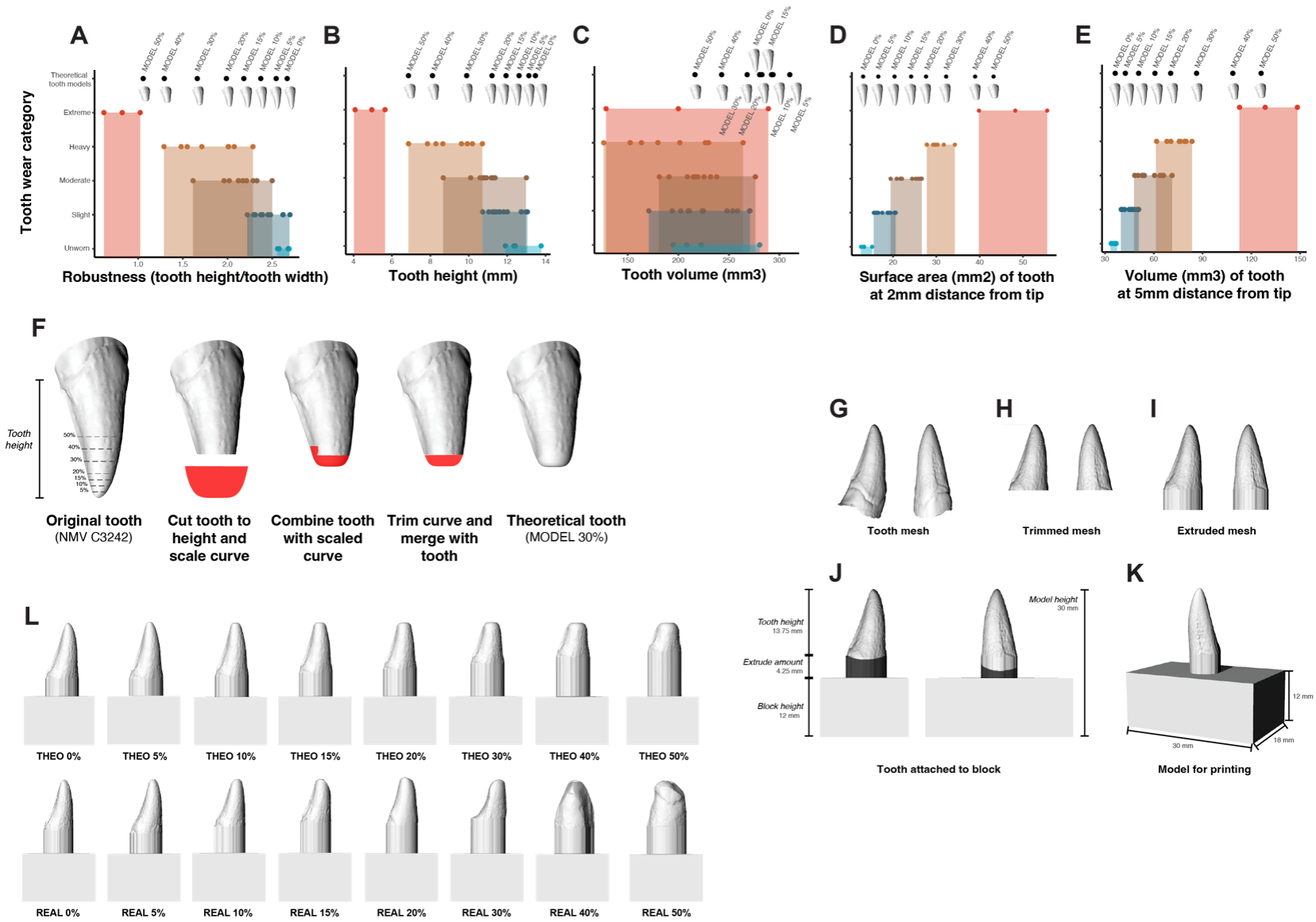


**Fig. S1.** Tooth wear categories and tooth shape metrics: (**A**) robustness, (**B**) tooth height, (**C**) tooth volume, (**D**) sharpness surface area, and (**E**) sharpness volume. (**F**) Theoretical tooth creation workflow shown on NMV C6242. Workflow for creating models for 3D printing as shown on tooth NMV C6242: (**G**) tooth mesh, (**H**) trimming, (**I**) extruding, (**J**) attaching to block, and (**K**) final model for printing.

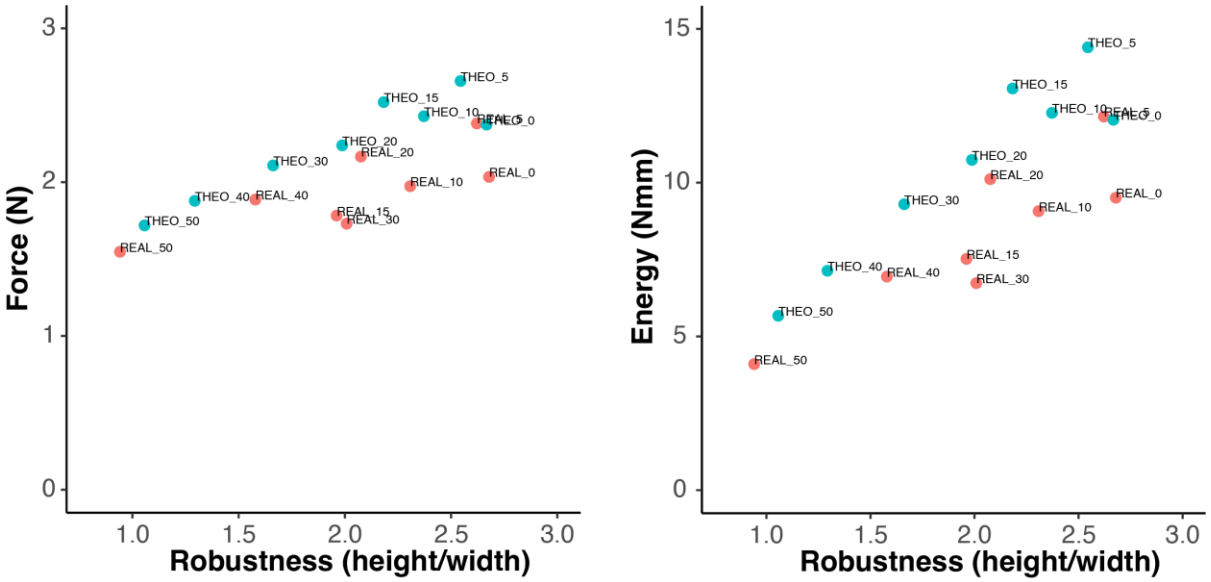


**Fig. S2.** Performance metrics (calculated from the whole bite) vs. robustness

**Table S1.** Specimen information for all canine teeth measured for this study including tooth wear category (from Pollock *et al.* 2021), and parameters measured: tooth height (mm), tooth width (mm), tooth robustness (tooth height/tooth width), tip sharpness: surface area 2 mm from tip ($mm^2$), tooth volume ($mm^3$), and tip sharpness: volume 5 mm from tip ($mm^3$).

Available for download at
https://journals.biologists.com/jeb/article-lookup/doi/10.1242/jeb.246925#supplementary-data

**Table S2.** Tooth puncture performance values calculated for each replicate for all tooth models tested. Including Maximum force (N) and energy (Nmm), calculated from the full run (displacement 18 mm), run chopped to tooth height (displacement equivalent to tooth height (mm)), and run chopped to 5 mm (displacement equivalent to 5 mm)).

Available for download at
https://journals.biologists.com/jeb/article-lookup/doi/10.1242/jeb.246925#supplementary-data

**Table S3.** Statistical output for all regressions undertaken in this study between performance metric(s) and aspects of tooth shape.

Available for download at
https://journals.biologists.com/jeb/article-lookup/doi/10.1242/jeb.246925#supplementary-data

**Table S4.** Raw force trace output (displacement (mm) and force (N)) for each tooth model replicate.

Available for download at
https://journals.biologists.com/jeb/article-lookup/doi/10.1242/jeb.246925#supplementary-data